

COVER PAGE

Document downloaded by @DAEL

Fri Nov 27 02:32:23 2026
For personal use

When automatic English translation is provided, only the original document is authentic.
The EAA cannot be held responsible of any translation error

Bibliographical reference

Sound Source Depth Estimation Based on Multipath Time Delay in Deep Water, Qiulong Yang and Kunde Yang, Acta Acustica **vol. 104** (Number 2), 2018, pp. 363-368

DOI
https://doi.org/10.3813/AAA.919178

ACTA ACUSTICA UNITED WITH ACUSTICA
Vol. 104 (2018) 363 – 368

DOI 10.3813/AAA.919178

Sound Source Depth Estimation Based on Multipath Time Delay in Deep Water

Qiulong Yang[1,2], Kunde Yang[1,2]
[1] School of Marine Science and Technology, Northwestern Polytechnical University, Xi'an 710072, China. ykdzym@nwpu.edu.cn
[2] Key Laboratory of Ocean Acoustics and Sensing (Northwestern Polytechnical University), Ministry of Industry and Information Technology, Xi'an 710072, China

Summary
In deep water, when the minimum time arrivals in all receiver depths are rowed and then fixed on a certain time on time delay-receiver depth plane, time delays of bottom reflection (BR) and surface-bottom-surface reflection (SBS) have a linear relationship with the receiver depth under the approximation condition. Besides, time delay arrivals of BR and SBS intersect at a receiver depth which is equal to the negative source depth. Based on the feature, a source depth estimation method with the multipath time delay difference is proposed. If the depths of receivers which are deployed vertically are known, the pair of time delays can be used to estimate the source depth. With the proposed method the source depth can be estimated successfully at a moderate range in deep water without complicated matched-field calculations in the simulations and experiments.

PACS no. 43.30.Cq, 43.60.Jn

1. Introduction

Passive source depth estimation has been studied for decades. Several methods for passive source depth estimation are introduced, such as matched-field processing (MFP), mode filter, matched mode, modal decomposition, wavenumber spectrum, interference pattern, time delay difference matching, cross-correlation matching and ray backpropagation procedure and so on.

Matched-field processing (MFP) method with Bartlett and minimum variance and a weighted-subspace-fitting (WSF) processors had been proposed for passive localization based on vertical line arrays in deep ocean[1, 2]. Based on the fact that a shallow acoustic source cannot excite the lowest order waveguide modes due to its evanescent amplitude dependence near the surface in a downward refracting ocean waveguide, a mechanism for differentiating a shallow acoustic noise source was provided [3]. A robustness source depth discrimination method was proposed based on mode filter and used the concept of trapped and free modes to build the trapped energy ratio [4, 5] in mode space . Yang utilized the modal decomposition to make a successful estimate of the range and depth in the Arctic Ocean. The energy (modal) of spectral peaks as a function of the receiver depth is used to estimate the source depth based on performing a wavenumber spectrum analysis of a narrowband signal received on vertical line array [6, 7]. If the hydrophone depths are known, the source depth can be estimated from three different arrival times by measuring the relative times of direct and surface-reflected arrivals at two hydrophones of arbitrary separation in the stratified ocean [8]. An extended Kalman filter [9] and an iterative, linearized Gauss-Markov inversion scheme [10] adopted the time delays between direct and surface-reflected acoustic arrivals recorded on hydrophones to passively estimate the transient source depth.

The side lobe curves appearing in the ambiguity surface of localization result are analytically expressed and are then used as indicators instead of the scanning point with the maximum power to localize a sound source in deep ocean based on a cross-correlation function matching technique[11, 12]. Reid and Zurk [13] introduced a modified Fourier-transform based method utilizing the depth-dependent interference between the direct and surface-reflected acoustic arrival for passive source depth estimation and exploited vertical line arrays deployed below the critical depth in deep ocean. A simplified method based on the angular spacing of the depth-harmonic interference nulls was also introduced for accurate sound source depth estimation in deep ocean [14]. What's more, Voltz [15] presented a new method for source localization which is based on a ray backpropagation procedure, and which exploits both the temporal and spatial characteristics of the multipath arrivals structure at a receiving sensor array.

In this paper, a simple method based on multipath time delay is proposed to estimate the source depth in deep water. The contents of this work are organized as follows. Section 2 introduces the theory and derivation of the source depth estimation method. Section 3 presents the simulations performed to estimate the source depth in deep ocean environment. Section 4 describes the experimental verification to demonstrate the feasibility of the estimation method. The conclusion and discussion are summarized in the final section.

2. The derivation of the source depth estimation method

From the view of ray theory, the eikonal equation describing the ray tracing of acoustic field is represented in terms of ray coordinate s as [16]

$$\tau(s) = \tau(0) + \int_0^s \frac{1}{c(s')}\,\mathrm{d}s', \tag{1}$$

where $\tau(s)$ is defined as the travel time through ray trajectory s. Assuming that the source emits a delta pulse, a series of pulses of with different time delays and amplitude decay through paths including direct path (D), surface reflection path (SR), bottom reflection path (BR), surface-bottom reflection (SB), bottom-surface reflection (BS) and surface-bottom-surface reflection (SBS) are received at the receiver.

The schematic of ray element is shown in Figure 1a in an oceanic waveguide. And the travel time along the ray element $\mathrm{d}s = |\mathrm{d}z/\sin\chi|$ is $\mathrm{d}t = \mathrm{d}s/c(z) = |\mathrm{d}z/[c(z)\sin\chi]|$, where χ. and $c(z)$ denote the grazing angle and sound speed at depth z, respectively. Then expressing $\mathrm{d}z$ in terms of $\mathrm{d}\chi$ by differentiating $\cos\chi(z)/c(z) = \text{const.}$, and thus the travel time in linear sound speed profile oceanic waveguide $c(z) = c_0(1 + az)$ (where ac_0 represents the sound speed gradient) along a ray between arbitrary depths z_1 and z_2 can be expressed as [17]

$$\begin{aligned} t &= \frac{1}{ac_0}\left|\int_{x_1}^{x_2}\frac{\mathrm{d}\chi}{\cos\chi}\right| \\ &= \frac{1}{ac_0}\left(\ln\frac{1+\sin\chi_1}{1-\sin\chi_1} - \ln\frac{1+\sin\chi_2}{1-\sin\chi_2}\right), \end{aligned} \tag{2}$$

Received 6 July 2017,
accepted 15 January 2018.

© S. Hirzel Verlag · EAA

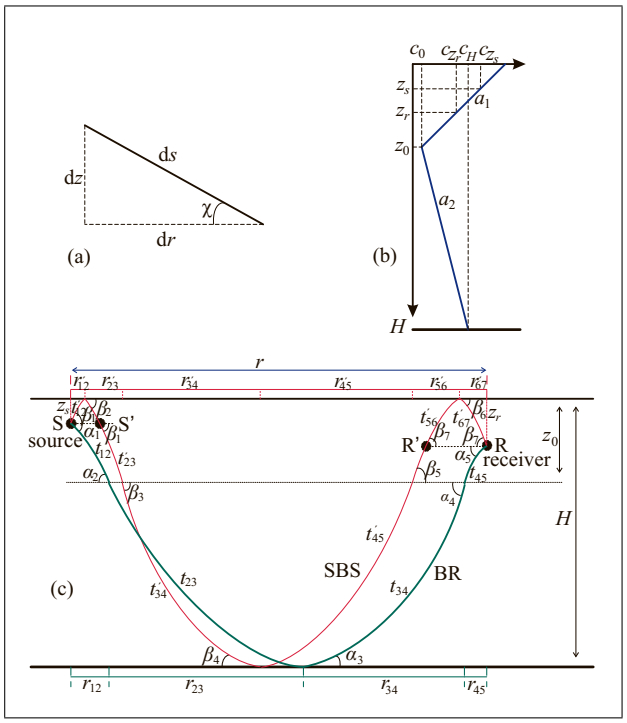

Figure 1. Ray elements and the schematic of multipath along BR and SBS in oceanic waveguide (a) ray elements (b) dual linear sound speed profile (c) schematic of multipath along BR and SBS.

where $\chi_1 = \chi(z_1)$, $\chi_2 = \chi(z_2)$. This is a well-known integral so that we have

$$\ln \frac{1+\sin x}{1-\sin x} \approx 2\left(x + \frac{x^3}{6} + \frac{x^5}{24} + \dots\right). \tag{3}$$

For an arbitrary infinitely small element of a ray one has $\mathrm{d}r = |\mathrm{d}z/\tan\chi|$. The total horizontal distance covered by the ray between arbitrary depths z_1 and z_2 can be expressed as

$$r = \left| \int_{z_1}^{z_2} \frac{\mathrm{d}z}{\tan\chi} \right|, \tag{4}$$

and thus the horizontal distance r_i covered by the ray in the ith layer can be expressed as

$$\begin{aligned} r_i &= \frac{1}{\cos\chi_{i-1}} \left| \frac{1}{g_i} \int_{\chi_{i-1}}^{\chi_i} \cos\chi \,\mathrm{d}\chi \right| \\ &= \frac{1}{\cos\chi_{i-1}} \left| \frac{1}{g_i} \left(\sin\chi_i - \sin\chi_{i-1} \right) \right|, \end{aligned} \tag{5}$$

where g_i is the relative sound velocity gradient in the ith layer, $g_i = (c_i - c_{i-1})/[c_{i-1}(z_i - z_{i-1})]$; χ_i and χ_{i-1} are the grazing angles at its boundaries. For the total horizontal distance covered by the ray we have $r = \sum_i r_i$. And in constant sound speed gradient oceanic environment, the horizontal distance r_i can be expressed as [18]

$$r_i = \frac{|z_i - z_{i-1}|}{\tan\left[\frac{1}{2}(\chi_i + \chi_{i-1})\right]}. \tag{6}$$

For the sake of simplicity, a dual linear sound speed profile as shown in Figure 1b is assumed in deep ocean. $a_1 c_0$ and $a_2 c_0$ represent sound speed gradient above and below sound channel axis depth z_0, where the sound speed is minimal and equal to c_0; and then the sound speed above and below sound channel axis can be expressed as $c_1 = c_0[1 + a_1(z_0 - z)]$ and $c_2 = c_0[1 + a_2(z - z_0)]$; z_s, z_r and H denote the source depth, the receiver depth and the water depth, respectively. The multipath eigenrays along paths of BR and SBS is shown in Figure 1c. α and β represent the grazing angle along sound ray through paths of BR and SBS. According to Snell law, the relationships between the grazing angle and sound speed along BR and SBS can be written as

$$\begin{aligned} &\frac{\cos\alpha_1}{c_0\left[1 + a_1(z_0 - z_s)\right]} = \frac{\cos\alpha_2}{c_0} \\ &= \frac{\cos\alpha_3}{c_0\left[1 + a_2(H - z_0)\right]} = \frac{\cos\alpha_4}{c_0} \\ &= \frac{\cos\alpha_5}{c_0\left[1 + a_1(z_0 - z_r)\right]} = A, \end{aligned} \tag{7}$$

$$\begin{aligned} &\frac{\cos\beta_1}{c_0\left[1 + a_1(z_0 - z_s)\right]} = \frac{\cos\beta_2}{c_0(1 + a_1 z_0)} \\ &= \frac{\cos\beta_3}{c_0} = \frac{\cos\beta_4}{c_0\left[1 + a_2(H - z_0)\right]} \\ &= \frac{\cos\beta_5}{c_0} = \frac{\cos\beta_6}{c_0(1 + a_1 z_0)} \\ &= \frac{\cos\beta_7}{c_0[1 + a_1(z_0 - z_r)]} = B, \end{aligned} \tag{8}$$

where A and B are constants; and $\alpha_2 = \alpha_4$, $\beta_3 = \beta_5$, $\beta_2 = \beta_6$. For each receiver of a vertical array, the horizontal distance covered by acoustic rays of BR and SBS must be equal to each other. The horizontal distance covered by the rays along BR and SBS can be written as

$$\begin{aligned} r_{\mathrm{BR}} &= r_{12} + r_{23} + r_{34} + r_{45} \\ &= r'_{12} + r'_{23} + r'_{34} + r'_{45} + r'_{56} + r'_{67} = r'_{\mathrm{SBS}}. \end{aligned} \tag{9}$$

Substituting Equation (6), Equation (7) and Equation (8) into Equation (9), and expanding the tangent of grazing angle in Taylor series, and the third power of grazing angle can be neglected. If $2r'_{12}$ and $2r'_{67}$ can be neglected compared to the total horizontal range r_{SBS} or r_{BR}, S' and R' are close to the source and receiver respectively. At the moment, the part of SBS path can be considered as a BR path. Finally, we can obtain $\alpha_1 \approx \beta_1$ or $A \approx B$ under the constraint condition, which can be written as

$$\begin{aligned} 2r'_{12} + 2r'_{67} &= \frac{2z_s}{2 + a_1(2z_0 - z_s)} + \frac{2z_r}{2 + a_1(2z_0 - z_r)} \\ &\ll \frac{2H - 2z_0}{2 + a_2(H - z_0)} + \frac{z_0 - z_s}{2 + a_1(z_0 - z_s)} \\ &\quad + \frac{z_0 - z_r}{2 + a_1(z_0 - z_r)}. \end{aligned} \tag{10}$$

Substituting Equation (2), Equation (3), and expanding the cosine and sine of grazing angle in power series, then the travel time along paths of BR and SBS can be written as

$$\begin{aligned} t_{\mathrm{BR}} &= t_{12} + t_{23} + t_{34} + t_{45} \\ &\simeq \frac{1}{a_1 c_0}\left[(2\alpha_2 - \alpha_1 - \alpha_5) + \frac{1}{6}\left(2\alpha_2^3 - \alpha_1^3 - \alpha_5^3\right)\right] \\ &\quad + \frac{2}{a_2 c_0}\left[(\alpha_2 - \alpha_3) + \frac{1}{6}\left(\alpha_2^3 - \alpha_3^3\right)\right] \\ &\simeq A\frac{16 - 8\pi}{\pi^3 - 8\pi}(2H - z_s - z_r) + \xi(a^3) + \xi(\alpha^4) \end{aligned} \tag{11}$$

and

$$\begin{aligned} t_{\mathrm{SBS}} &= t'_{12} + t'_{23} + t'_{34} + t'_{45} + t'_{56} + t'_{67} \\ &\simeq \frac{1}{a_1 c_0}\Big[\big(\beta_1 + 2\beta_3 + \alpha_7 - 4\beta_2\big) \\ &\qquad + \frac{1}{6}\big(2\beta_1^3 + 2\beta_3^3 - \alpha_7^3 - 4\beta_2^3\big) \\ &\quad + \frac{2}{a_2 c_0}\Big[\big(\beta_3 - \beta_4\big) + \frac{1}{6}\big(\beta_3^3 - \beta_4^3\big)\Big] \\ &\simeq B\frac{16-8\pi}{\pi^3 - 8\pi}\big(2H + z_s + z_r\big) + \zeta(\beta^3) + \zeta(\beta^4), \end{aligned} \tag{12}$$

where

$$\begin{aligned} \xi(\alpha^3) &= \frac{\pi^2 - 16}{6(\pi^2 - 8)}\frac{1}{c_0}\Big[\frac{1}{a_1}\big(2\alpha_2^3 - \alpha_1^3 - \alpha_5^3\big) \\ &\qquad + \frac{1}{a_2}\big(2\alpha_2^3 - 2\alpha_3^3\big)\Big], \\ \xi(\alpha^4) &= \frac{\pi}{6(\pi^2 - 8)}\Big[\frac{1}{a_1}\big(2\alpha_2^4 - \alpha_1^4 - \alpha_5^4\big) \\ &\qquad + \frac{1}{a_2}\big(2\alpha_2^4 - 2\alpha_3^4\big)\Big], \end{aligned} \tag{13}$$

$$\begin{aligned} \zeta(\beta^3) &= \frac{\pi^2 - 16}{6(\pi^2 - 8)}\frac{1}{c_0}\Big[\frac{1}{a_1}\big(\beta_1^3 + 2\beta_3^3 + \beta_7^3 - 4\beta_2^3\big) \\ &\qquad + \frac{1}{a_2}\big(2\beta_3^3 - 2\beta_4^3\big)\Big], \\ \zeta(\beta^4) &= \frac{\pi}{6(\pi^2 - 8)}\frac{1}{c_0}\Big[\frac{1}{a_1}\big(\beta_1^4 + 2\beta_3^4 + \beta_7^4 - 4\beta_2^4\big) \\ &\qquad + \frac{1}{a_2}\big(2\beta_3^4 - 2\beta_4^4\big)\Big]. \end{aligned} \tag{14}$$

According to Equation (13) and Equation (14), the time delay arrivals of BR and SBS can be considered to have a linear relationship with receiver depth. Therefore, solving the intersection point of the time delay arrivals of BR and SBS is equivalent to finding the minimum time delay difference between BR and SBS. And thus the time delay difference between BR and SBS can be expressed as

$$\tau_{\mathrm{BR-SBS}} = \big|t_{\mathrm{BR}} - t_{\mathrm{SBS}}\big|. \tag{15}$$

Substituting Equation (11) and Equation (12) into Equation (15), and assuming that $\tau_{\mathrm{BR-SBS}}$ is equal to 0, when the third and fourth power of grazing angle can be neglected (approximation condition: $\xi(\alpha^3)$, $\xi(\alpha^4)$, $\zeta(\beta^3)$ and $\zeta(\beta^4)$ are approximately equal to zeroes;), the solution of Equation (15) is represented as

$$z_s = -z_r. \tag{16}$$

The result in Equation (16) implies that on τ–z plane (the time delay – receiver depth plane) the time delay arrivals of BR and SBS intersect at a receiver depth which is equal to the negative source depth, where the time delay difference of BR and SBS is minimal. Based on this feature, the intersection points of BR and SBS can be used to estimate the source depth. Then the theory is extended to range-independent deep ocean waveguide when the approximation condition is met. For plane wave approximation, the time delay arrivals of BR and SBS have a linear relationship with the receiver depth. And the intersection points of BR and SBS can be used to estimate the source depth in deep ocean under the approximation condition. What's more, the source depth estimation method has no close relationship with the sound speed profile but has close relationship with the accuracy of extracting of time delay arrivals of BR and SBS.

3. Simulation results

The sound speed profile (SSP) adopted in the simulation is obtained from experimental measurements in a deep ocean area of the South China Sea in August 2014. The mixed layer depth is approximately 70 m. The sound channel axis and the sea depth are about 1100 m and 4000 m as shown in Figure 3. Sediment sound speed, sediment density, and sediment attenuation coefficient are approximately 1560 m/s, 1.30 g/cm^3 and 0.10 dB/λ. based on core data, respectively. And the seabed terrain is flat approximately. It is assumed that the acoustic channel is range-independent waveguide. BELLHOP [19] acoustic code is utilized to calculate the multipath time delay arrivals and demonstrate the feasibility of proposed source depth estimation method in deep ocean.

The number of rays used to find eigenrays is determined by procedure automatic based on environmental parameters. The SSP was input at depths of from 0 m to 1200 m in step of 10 m, from 1200 m to 4000 m in step of 50 m. The multipath time delay arrivals for source depths of 10 m, 50 m and 300 m at a range of 13.2 km are shown in Figure 2a, 2b and 2c. Time delay arrivals of SB, BS, BR and SBS can be distinguished clearly at the receiver range of 13.2 km. Here all the time delays arrivals are time delay differences relative to the minimum arrival time which is rowed and then fixed on the first second and travels along path of direct path. The sound trace length of BR is smaller than the one of SBS, so the time delay arrivals of BR is smaller than the counterpart of SBS. Approximately, time delay arrivals of BR and BS are parallel to those of SB and SBS respectively. Furthermore, time delay arrivals of BR and BS, SB and SBS intersect at the surface. Based on the theory above, the time delay arrivals of BR and SBS can be considered to have a linear relationship with the receiver depth. The intersection points are denoted by a black square when the time delay arrivals of BR and SBS are extended and extrapolated toward the negative receiver depth linearly based on least mean square error (LMSE) criterion. And the source depth is the absolute value of the intersect point and estimated successfully.

The source depth estimation results in simulation with the proposed method for source depths of 10 m, 50 m and 300 m are shown in Figure 2d, 2e and 2f. All the source depths can be estimated correctly for the receiver range of 1–25 km. However, the estimation results slightly deviate from the real source depth when the range is larger than 20 km. The maximum biases are less than 5 m for source depths of 10 m and 50 m, and the maximum bias is less than 10 m for source depth of 300 m. For all the source depths, the maximum biases are all less than 10% of the real source depths. As the receiver range increases, the grazing angle with respective to horizontal direction decreases, and ray refraction will have important effects on source depth estimation. At the moment, then the time delay arrivals of BR and SBS do not exhibit completely linear relationship with receiver depth but process a quasi-linear relationship. The estimation error is sensitive to the extracted accuracy of time delay arrivals along BR and SBS. Above all, the proposed method can be used to estimate the source depth in deep ocean with the time delay arrivals of BR and SBS.

4. Experiment verification

In 2014, an experiment of sound propagation was conducted in a deep ocean area of the South China Sea (SCS). Figure 3a shows the schematic of experiment and the measured sound speed profile. The oceanic waveguide is an uncompleted acoustic channel

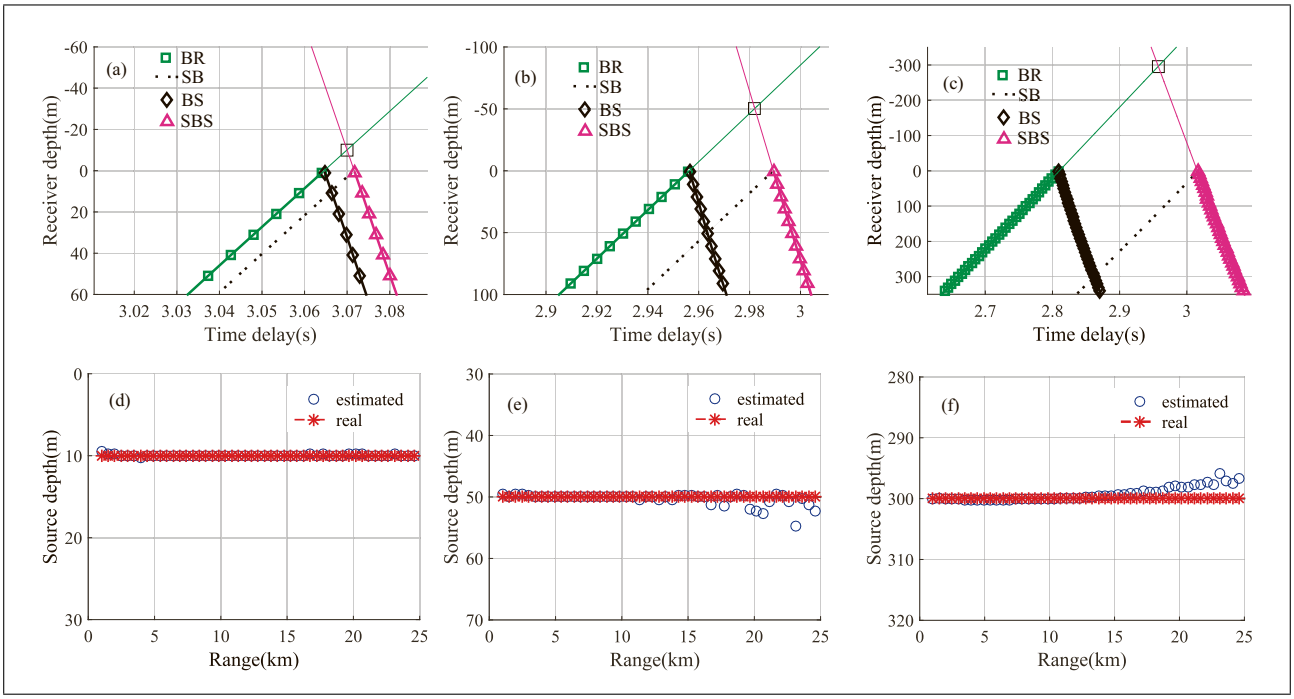

Figure 2. Multipath time delay arrival structure and source depth estimation results with time delay between BR and SBS for different source depths at range of 13.2 km: (a) SD = 10 m (b) SD = 50 m (c) SD = 300 m (d) SD = 10 m (e) SD = 50 m (f) SD = 300 m.

without critical depth, because the sound speed at the bottom is less than the sound speed on the sea surface. Sea depth is approximately 4000 m, and the seabed terrain is relatively flat. The receiver vertical array was moored by a weight block near the bottom and composed of 16 distributed hydrophones that sampled and recorded acoustic signal solely. The depth vertical line array spanned from 110–820 m with different intervals. The sample rate and the sensitivity of hydrophones was 48 kHz and −180 dB re 1 V/μPa, respectively. The broadband explosive sources with 1 kg TNT and nominal detonation depth of 50 m and 300 m were dropped by turns from the research ship away from the receiver array. According to the proposed method, the time delay arrivals of BR and SBS are regarded to have a linear relation with the receiver depth. Cross correlation method and linear fitting method based on least mean squares error criterion (LMSE) can be used to extract and extend the time delay arrivals of BR and SBS [20]. The hydrophone depths can be obtained from the temperature and depth sensors fixed on the mooring of receiver array. In the period of source depth estimation, the array tilt caused by the ocean current is also considered, and the receiver depths are corrected to reduce and eliminate the error.

Because of some reasons, signals received by fourteen hydrophones were utilized for source depth estimation method verification. The maximum receiver depth of the fourteen hydrophones was less than 500 m as shown in Figure 4. Figure 4a, 4d show the multipath time delay arrival structure at a range of approximately 5.8 km in the experiment for nominal source depths of 50 m and 300 m, respectively. Signals received on the vertical line array are used to analyze the multipath time delay arrivals in the deep ocean. Consistent with the results in simulation, the multipath time delay arrivals, including D, SR, BR, BS, SB and SBS, can be distinguished clearly due to high signal-to-noise ratio (SNR) of explosive charges. The multipath time delay arrivals are relative to the minimum arrival time, which is time arrival through direct path and is rowed and then fixed on the first second. Figure 4b, 4e show the local view denoted by black dash

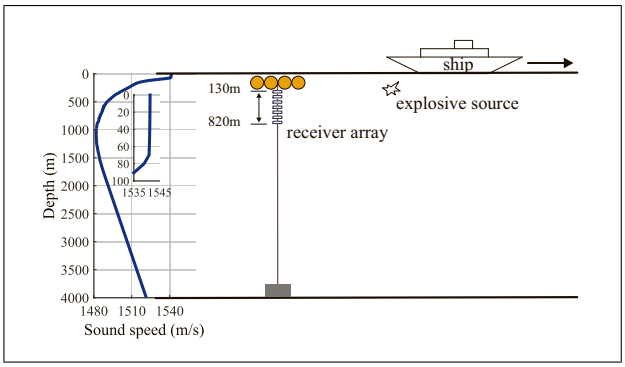

Figure 3. The measured sound speed profile and schematic of experiment in SCS2014.

square in 4a, 4c, the local view shows the linear relationship and multipath time delay arrivals of signals received on vertical array more clearly. Approximately, the time delay arrivals of BR and BS are parallel to those of SB and SBS respectively. Furthermore, the time delay arrivals of BR and BS, and those of SB and SBS intersect at the sea surface. Based on the fact that the length of trace through path of BR is less than the one of SBS, the time delay of BR is smaller than that of SBS. The time delay arrivals of BR and SBS are extracted at each hydrophone using cross correlation and linear regression based on least mean square error (LMSE) criterion. Then the lines of time delay arrivals through paths of BR and SBS with respect to receiver depth are extended and extrapolated towards the negative receiver depth and the intersect points are denoted by black squares. Finally, the vertical axis values of intersect points are equal to the negative source depths whose absolute value are the source depths.

The source depth estimation results for the range of 5–27 km and the source depths of 50 m and 300 m in the experiment are shown in Figure 4c and 4f with the proposed method. Compared with nominal depth, which is a preset depth before the explosive

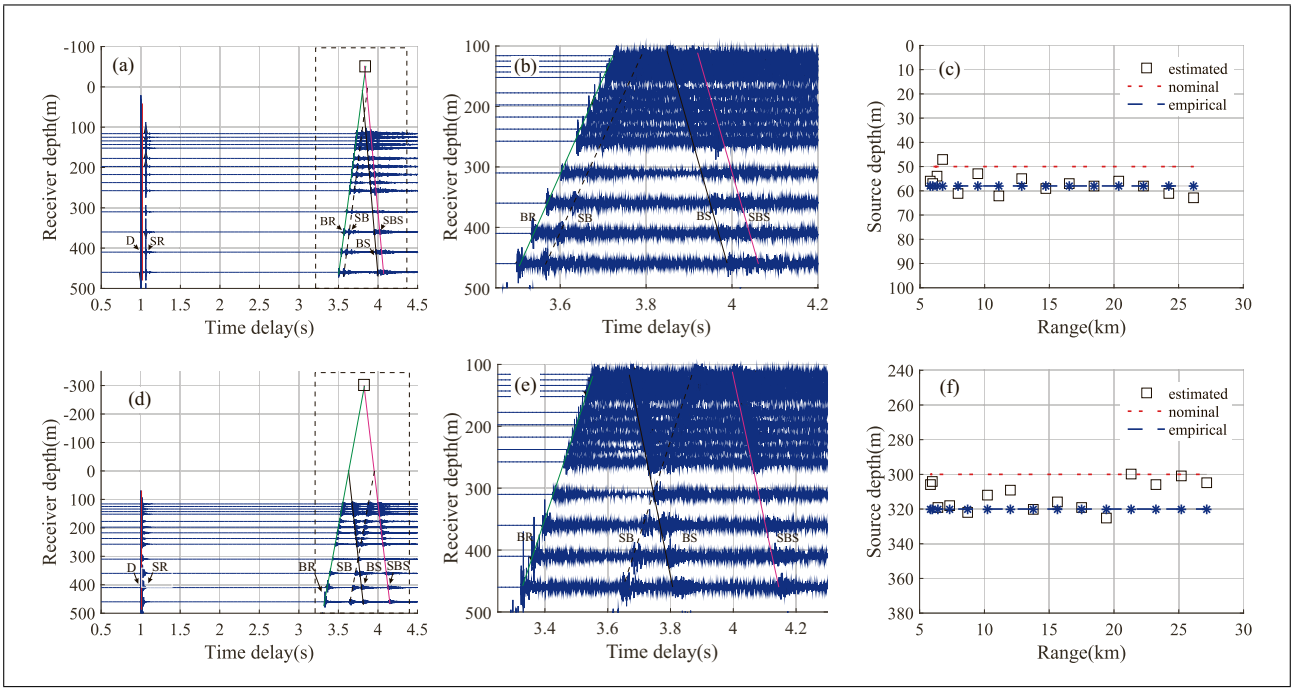

Figure 4. Experiment verification results. (a)(b) Multipath time delay arrival structure and local view time delay arrivals for source depth of 50 m at range about 5.8 km. (c) Estimation results for source depth of 50 m. (d)(e) Multipath time delay arrival structure and local view time delay arrivals for source depth of 300m at range about 5.8 km (f) Estimation results for source depth of 300 m.

charges leaving the factory, the estimation results deviate from the nominal depth, and the maximum bias is about 10 m for the source depth of 50 m. And the estimated source depth is deeper than the nominal source depth for the range of 5–27 km. But for the nominal source depth of 300 m, the maximum bias is about 30 m, and the estimated source depth is also deeper than the nominal source depth for the range. For the explosive sources, the nominal source depth may not be accurate and may not be the real underwater explosive depth. The actual explosion depth is not known and may deviate from the nominal depth. The actual detonation depth can be expressed by an empirical relationship based on the bubble pulse period [21]. The bubble period is given by the relationship

$$T_i = K_i w^{1/3} \left(z_0 + 10\right)^{-5/6}, \tag{17}$$

where T_i is the period of the ith bubble pulse in seconds and K_i is a constant which has the values $K_i = 2.11$,1.48 and 1.20 respectively for the first three pulse; w and z_0 denote the charge weight and the explosion depth, respectively.

Figure 5 shows the signal waveform of explosive charges for source depths of 50 m and 300 m during source level measurement in the experiment. The time delay difference between shock pulse and first bubble pulse is named first bubble pulse period. A total of ten explosive charges for each nominal depth were used during the period of the source level measurement in the experiment. The averaged first bubble pulse periods for the nominal depth of 50 m and 300 m are 62.6 ms and 16.8 ms based on measurement data, respectively. Therefore, the detonation depths are corrected to be 58 m and 320 m with the empirical relationship for the nominal depth of 50 m and 300 m approximately. The corrected depths are denoted by empirical depth that is considered to be more credible than the nominal depth. The estimation results are in agreement with empirical depths. At a moderate range, the source depth can be estimated successfully. The maximum bias is less than 10% for both source depths of 50 m and 300 m.

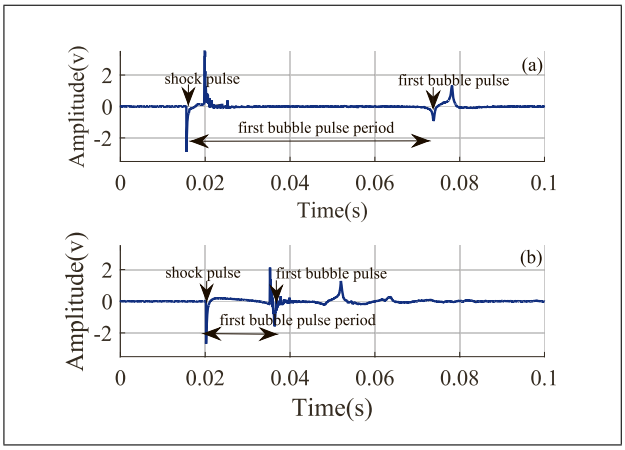

Figure 5. The signal waveform of explosive charges for source depths of (a) 50 m and (b) 300 m during source level measurement in SCS2014.

The factors inducing estimation errors are represented as follows: first, because of the scattering of the surface and the bottom, the slopes of the time delay arrivals of BR and SBS are not extracted accurately in the experiment. Second, the real source detonation depths are unknown and may diverge from the nominal depths. Third, the deep ocean acoustic channel in the experiment is not a completely range-independent waveguide. Finally, the time delay arrivals of BR and SBS fail to have a completely linear relation with the receiver depth but process a quasi-linear or piecewise-linear relation due to ray fraction and decreasing grazing angle.

5. Conclusion

In this context, a method for source depth estimation in deep ocean is proposed and demonstrated with simulations and experiments. The method performs well in both simulations and

experiments at a moderate range in deep water. It is simple and performing complicated matched-field calculations sensitive to environment parameters is unnecessary in the range-independent deep ocean. Before estimating the source depth, it is essential to consider the array tilt and correct the receiver depth based on pressure sensors. Under the approximation condition that the third and fourth power of grazing angle can be neglected, then the time delay arrivals of BR and SBS have a linear relationship with the receiver depth. Besides, the time delay arrivals of BR and SBS intersect at a receiver depth, which is equal to the negative source depth where the time delay difference between BR and SBS is minimal. Then the vertical axis value of intersect point can be used to estimate the source depth on time delay-receiver depth plane. The estimation errors are sensitive to the slopes of the pair of time delay arrivals. Therefore, the key to estimate the source depth correctly is to extract the time delay arrivals accurately. At least, double hydrophones are needed and deployed vertically, if their depths are known, the source depth can also be estimated successfully with the proposed method by only measuring the time delay difference of BR and SBS. The method is valid for explosive sources with high SNR, but for other sources with low SNR, the method will be demonstrated in the future work because time delay arrivals of BR and SBS cannot be extracted accurately.

Acknowledgement

This work was supported by the National Natural Science Foundation of China (Grant No. 11174235). Conflict of interest: The authors declare that they have no conflict of interest.

References

[1] J. M. Q. D. Tran, W. S. Hodgkiss: Matched-field processing of 200hz continuous wave (cw) signals. J. Acoust. Soc. Am. **89** (1991) 745–755.

[2] R. Duan, K. D. Yang, Y. L. Ma, B. Lei: A reliable acoustic path: Physical properties and a source localization method. Chinese Physics B **21** (2012) 124301.

[3] V. E. Premus, M. N. Helfrick: Use of mode subspace projections for depth discrimination with a horizontal line array: theory and experimental results. J. Acoust. Soc. Am. **133** (2013) 4019–4031.

[4] E. Conan, J. Bonnel, T. Chonavel, B. Nicolas: Source depth discrimination with a vertical line array. J. Acoust. Soc. Am. **140** (2016) EL434–EL440.

[5] T. C. Yang: A method of range and depth estimation by modal decomposition. J. Acoust. Soc. Am. **82** (1987) 1736–1745.

[6] T. C. Yang, W. Xu: Data-based depth estimation of an incoming autonomous underwater vehicle. J. Acoust. Soc. Am. **140** (2016) EL302–EL306.

[7] D. B. Reeder: Clutter depth discrimination using the wavenumber spectrum. J. Acoust. Soc. Am. **135** (2014) EL1–EL7.

[8] E. K. Skarsoulis, M. A. Kalogerakis: Ray-theoretic localization of an impulsive source in a stratified ocean using two hydrophones. J. Acoust. Soc. Am. **118** (2005) 2934–2943.

[9] R. Duan, K. D. Yang, Y. L. Ma, Q. L. Yang, H. Li: Moving source localization with a single hydrophone using multipath time delays in the deep ocean. J. Acoust. Soc. Am. **136** (2014) EL159–EL165.

[10] E. K. Skarsoulis, S. E. Dosso: Linearized two-hydrophone localization of a pulsed acoustic source in the presence of refraction: theory and simulations. J. Acoust. Soc. Am. **138** (2015) 2221–2234.

[11] E. K. Westwood, D. P. Knobles: Source track localization via multipath correlation matching. J. Acoust. Soc. Am. **102** (1997) 2645–2654.

[12] Z. Lei, K. Yang, Y. Ma: Passive localization in the deep ocean based on cross-correlation function matching. J. Acoust. Soc. Am. **139** (2016) EL196–EL201.

[13] R. McCargar, L. M. Zurk: Depth-based signal separation with vertical line arrays in the deep ocean. J. Acoust. Soc. Am. **133** (2013) EL320–EL325.

[14] G. P. Kniffin, J. K. Boyle, L. M. Zurk, M. Siderius: Performance metrics for depth-based signal separation using deep vertical line arrays. J. Acoust. Soc. Am. **139** (2016) 418–425.

[15] P. Voltz, I. Lu: A time-domain backpropagation ray technique for source localization. J. Acoust. Soc. Am. **95** (1994) 805–812.

[16] F. B. Jensen, W. A. Kuperman, M. B. Porter, et al.: Computational ocean acoustics. AIP press, New York, 2011.

[17] Y. L. M. Brekhovskikh, P. Lysanov: Fundmentals of ocean acoustics. AIP press, New York, 2003.

[18] B. S. Liu, J. Y. Lei: Principle of underwater sound (in Chinese). Harbin Engineering University Press, 2010. 86-91.

[19] M. B. Porter: The BELLHOP manual and user's guide: preliminary draft. http://oalib.hlsresearch.com/Rays/HLS-2010-1.pdf, 31 January 2011.

[20] K. D. Yang, Q. L. Yang, X. L. Guo, R. Cao: A simple method for source depth estimation with multi-path time delay in deep ocean. Chin. Phys. Lett. **33** (2016) 124302.

[21] N. R. Chapman: Measurement of the waveform parameters of shallow explosive charges. J. Acoust. Soc. Am. **78** (1985) 672–681.